



**MAPP
ATBD**

AVHRR compatible NDVI

Title: AVHRR compatible NDVI

Doc. no: MAPP-ATBD-NDVI

Issue: 1

Revision: 0

Date: 07/06/99

Author: K. P. Günther, S. Maier
DLR
Institute of Optoelectronics
Department of Optical Remote Sensing
D - 82 230 - Wessling
Germany



**AVHRR compatible
NDVI
ATBD**

Doc. ID : MAPP-ATBD-NDVI
Name : NDVI
Issue : 1 Rev.: 0
Date : 08/06/99
Page : ii

internal Distribution

Name

Quantity

external Distribution

Name

Quantity

Change Record

Issue

Revision

Date

Description

Change pages



**AVHRR compatible
NDVI
ATBD**

Doc. ID : MAPP-ATBD-NDVI
Name : NDVI
Issue : 1 Rev.: 0
Date : 08/06/99
Page : iii

Table of Contents

1. INTRODUCTION..... 1
1.1 ALGORITHM IDENTIFICATION 1

2. ALGORITHM OVERVIEW..... 1
2.1 AVHRR PROCESSING SCHEME AT DFD FOR THE GENERATION OF NDVI..... 1
2.2 MODIS_NDVI 2

3. ALGORITHM DESCRIPTION..... 3
3.1 THEORETICAL DESCRIPTION 3
3.1.1 *Mathematical Description of the Algorithm*..... 3
3.1.1.1 Modeling the AVHRR_reflectance3
3.1.1.2 Modeling MERIS_reflectance.....4
3.1.1.3 Simulation of AVHRR channels by MERIS channels4
3.1.1.4 MERIS parameter and sun position6
3.1.1.5 Simulation of leaf reflectance.....8
3.1.1.6 Simulation of canopy reflectance.....9
3.1.1.7 Test of the correlation of MERIS_NDVI with AVHRR_NDVI.....11
3.2 PRACTICAL CONSIDERATIONS..... 12
3.2.1 *Numerical computation considerations* 13
3.2.2 *Calibration and Validation*..... 13
3.2.3 *Exception Handling* 13
3.2.4 *Output Products*..... 13

4. ERROR BUDGET ESTIMATES 13

5. REFERENCES 14

6. MAPP DATA PRODUCT SUMMARY SHEET 15

7. ACKNOWLEDGEMENT 15



1. INTRODUCTION

1.1 Algorithm Identification

1. Daily AVHRR compatible NDVI map based on full resolution MERIS level 1b data
2. Weekly AVHRR compatible NDVI map based on product number 1.
3. Monthly AVHRR compatible NDVI map based on product number 2.

2. ALGORITHM OVERVIEW

The "Normalized Difference Vegetation Index" (NDVI) is widely used to estimate changes in vegetation state. NDVI was originally used as a measure of green biomass (Tucker et al., 1986). It got a solid theoretical basis as a measure of the solar photosynthetic active radiation absorbed by the canopy (Sellers, 1985). The NDVI involves relating the reflectance ρ_1 (or radiance) in the red range (near 675 nm) and in the NIR range (termed ρ_2) to vegetation variables such as leaf area index (LAI), canopy cover, and the concentration of the total chlorophyll. Green vegetation has low reflectance near 675 nm and the relationship of NDVI vs. chlorophyll (Chl) saturates for low Chl content (higher than 10 $\mu\text{g}/\text{cm}^2$ for intact bean leaves: Buschmann and Nagel, 1993, 3-5 $\mu\text{g}/\text{cm}^2$ for maple and chestnut leaves: Gitelson and Merzlyak, 1994; 1996; less than 3-5 $\mu\text{g}/\text{cm}^2$ for tobacco leaves: Lichtenthaler et al., 1996 and even less than 2 $\mu\text{g}/\text{cm}^2$ for sugar maple leaves (Vogelmann 1994).

Thus, NDVI is sensitive to low Chl contents, to low fraction of vegetation cover and, as a result, to low level of absorbed photosynthetic active solar radiation (Gitelson et al., 1996; Gitelson and Merzlyak, 1996; Yoder and Waring, 1994). But it is not sensitive at higher Chl contents or to rate of photosynthesis for large vegetation coverage.

For land surfaces dominated by vegetation, the NDVI values normally range from 0.1 to 0.7 during the growth season, the higher values being associated with greater density and greenness of the plant canopy. Atmospheric effects, such as Rayleigh scattering at molecules, Mie scattering at aerosols, gaseous absorption by atmospheric constituents and sub-pixel-sized clouds, all tend to increase the value of channel 1 with respect to channel 2 and reduce the values of the computed vegetation indices.

2.1 AVHRR processing scheme at DFD for the generation of NDVI

The visible and near infrared data of AVHRR (channels 1 and 2) are calibrated from raw counts to % technical albedo according to the time-adjusted calibration coefficients or to pre-flight values. The calibration coefficients have been updated once a month by NOAA/NESDIS. No atmospheric corrections are presently performed. The derivation of the "Normalized Difference Vegetation Index" is performed according to the following algorithm:

$$\text{AVHRR_NDVI} = (\rho_2 - \rho_1) / (\rho_1 + \rho_2)$$

ρ_i are the surface reflectances given in technical albedo (%).

 DLR	<h1>MERIS</h1>	Doc : MAPP-ATBD-NDVI Name : NDVI Issue : 1 Rev : 0 Date : 08/06/99 Page : 2
-------------------------------------------------------------------------------------------------	----------------	-----------------------------------------------------------------------------------------------------------------------------------

For the AVHRR on NOAA 15 the two channels are centered at $\lambda_1 = \sim 642 \text{ nm} \pm 55 \text{ nm}$ and at $\lambda_2 = \sim 856 \text{ nm} \pm 125 \text{ nm}$. The spatial resolution of AVHRR is about 1000 m (at nadir direction).

A couple of cloud/water tests are performed to ensure that only NDVI values over cloud-free land surfaces are derived. These tests are based on typical spectral characteristics of land, clouds and water. The selection scheme is based not only channel 1 and 2 but also channel 4 and 5. These two latter channels deliver information about the temperature of land, water and clouds. In addition the observation zenith angle is also taken into account.

Once, the NDVI is calculated, all data are remapped into a stereographic projection with a geometric resolution of 1.1132 km at map center applying "nearest neighbor re-sampling." Daily maps are composed on the maximum NDVI value basis at every pixel's position. The weekly and monthly images are calculated by taking the maximum NDVI value at every pixel's position over the time period regarded. A land/sea mask (WDB-II) is applied to every image to mask the remaining NDVI values over the ocean areas.

The NDVI values are scaled to a 8-bit integer format (values from 0 -255) with the following interpretation:

Parameter	Value range	Integer scaling
<i>Water</i>	-	0
<i>Cloud (or no data)</i>	-	255
NDVI_MIN	-0.09968454	1
NDVI_MAX	0,7	254

The resolution is 0.0031546. The NDVI value range is from -0.09968454 to 0.7. High quality products are derived from cloud-free land pixels after supervised processing.

NDVI is derived from 3 daily afternoon passes, which are processed to a daily maximum chart. From these daily charts, weekly and monthly maximum maps are derived. Therefore a weekly composite normally consists of 21 passes, a monthly map consists of about 90 passes.

2.2 MODIS_NDVI

The primary interests of NASA Earth Observing System (EOS) program is to study the role of vegetation in large-scale processes (on a global scale). In order to fulfil this task, the biophysical properties of vegetation together with their spatial and temporal variations are required. Remote sensing data as e.g. the derived NDVI offer the opportunity to monitor and quantify the status of vegetation. Therefore, NASA has announced to produce a vegetation index on a global scale based on MODIS data. This vegetation index is according to NASA statements the NDVI. This parameter is regarded as a "continuity index" to the existing NOAA-AVHRR derived NDVI. The long-term NDVI data derived from NOAA-AVHRR should be extended by MODIS data to provide a data continuity for operational monitoring studies.

The MODIS_NDVI will be calculated according to the well known algorithm:

$$\text{MODIS_NDVI} = (\rho_2 - \rho_1) / (\rho_1 + \rho_2)$$

ρ_i are the bi-directional surface reflectances generated from level 1b, calibrated at sensor radiances, masked for clouds, cloud shadows and atmospherically corrected with regard to aerosols, Rayleigh scattering and ozone absorption.

The two channels are centered at $\lambda_1 = 648 \text{ nm} \pm 25 \text{ nm}$ and at $\lambda_2 = 858 \text{ nm} \pm 17.5 \text{ nm}$. The spatial resolution will be 250 m (at nadir direction) with a radiometric resolution of 12 bit.

A spatial and temporal gridded MODIS_NDVI (level 3) derived from the daily MODIS_NDVI (level 2) is planned. The gridded vegetation index is a 8, 16 and 30 days spatial and temporal, re-sampled

	<h1>MERIS</h1>	Doc : MAPP-ATBD-NDVI Name : NDVI Issue : 1 Rev : 0 Date : 08/06/99 Page : 3
-----------------------------------------------------------------------------------	----------------	-----------------------------------------------------------------------------------------------------------------------------------

product to provide cloud-free, atmospherically corrected and nadir adjusted maps at nominal spatial resolution of 250 m. The compositing algorithm is based on the maximum - NDVI criteria.

Summarizing, the MODIS_NDVI is not a “continuity index” for the AVHRR_NDVI because the new vegetation index is based on atmospherically corrected and nadir adjusted data. In addition, differences may occur due to the different sensor specifications. For the AVHRR_NDVI broad spectral channels are used while the MODIS_NDVI is based on relative small spectral channels.

3. ALGORITHM DESCRIPTION

3.1 Theoretical Description

3.1.1 Mathematical Description of the Algorithm

The “Normalized Difference Vegetation Index” (NDVI) for the AVHRR sensor on board of the NOAA satellites is defined by the following equation:

$$AVHRR_NDVI = (\rho_2 - \rho_1) / (\rho_1 + \rho_2)$$

With ρ_1 and ρ_2 as the technical albedo (in %) of channel 1 (visible) and 2 (infrared) of AVHRR respectively. The technical albedo is calculated from the raw data (digital number) by applying the calibration coefficients delivered for the appropriate satellite (in the moment NOAA-12, NOAA-14 and NOAA-15).

For NOAA-15 launched on May 15th, 1998, and being operational on November 2nd, 1998, the pre-launch coefficients are used while for NOAA-14 launched on January 6th, 1995, and being operational on January 19th, 1995, time-adjusted calibration coefficients are needed. The calibration for all AVHRR sensors shows a linear relationship between raw data and technical albedo and was determined prior to launch.

In order to derive from MERIS data a MERIS_NDVI which can be regarded as a real “continuity index” the following equation should hold:

$$AVHRR_NDVI = MERIS_NDVI$$

The interest of the following section is to show that a MERIS_NDVI can be developed which is valid for typical surface conditions (different leaf parameters, different canopy structures) and most observation geometries occurring during a year for MERIS passing the M1 grid. The M1 grid is the area where most MAPP products should be valid.

3.1.1.1 Modeling the AVHRR_reflectance

The AVHRR_NDVI is defined in section 2.1 and 3.1.2, while the technical albedo or reflectance is given by:

$$\rho_i = cal_i * DN_{AVHRRi}$$

The calibration coefficients cal_i are given for all AVHRR sensors by NOAA/NESDIS and updated since November 1996 once a month. The parameter DN_{AVHRRi} is the digital number or count for each channel.

In turn the digital count of each spectral channel can be calculated according to:

$$DN_{AVHRRi} = gain_i * \int \tau_{AVHRRi}(\lambda) * L(\lambda) d \lambda$$

The sensor specific parameters $gain_i$ summarize the electronic factors for each channel i and are regarded as wavelength independent. For the moment, these parameters are set to 1. The variable $L(\lambda)$ represents the upward radiance entering the optics of the sensor. $L(\lambda)$ can be regarded as the reflected radiance from the ground superimposed by atmospheric radiance components as e.g. Rayleigh and Mie scattering component. For the AVHRR sensors the transmissions function $\tau_{AVHRRi}(\lambda)$ of each channel is given by NOAA/NESDIS. Thus, the following can be written:

$$\rho_i = \int \tau_{AVHRRi}(\lambda) * cal_i * L(\lambda) d \lambda$$

The product $cal_i * L(\lambda)$ may be regarded as the reflectance in channel i measured with an ideal sensor having a rectangular transmission function of 100% and 0% outside the transmission band.

3.1.1.2 Modeling MERIS_reflectance

Analogue to the modeling of the reflectance of each AVHRR channel, the reflectance of each MERIS channel can be calculated according to:

$$\rho_i^* = cal_i^* * gain_i^* \int \tau_{MERIS,i}(\lambda) * L(\lambda) d \lambda$$

The factors with an asterisk will indicate all MERIS related parameters. Due to the fact, that the main parameters as e.g. the transmission function of each channel, the gain factors and the calibration factors for MERIS are not yet known, the following assumptions are made:

- The transmission function of each MERIS channel is represented by a Gaussian function with the maximal transmission of 1 at the center wavelength and bandwidth given by ESA.
- The calibration and gain parameters are set to 1.

3.1.1.3 Simulation of AVHRR channels by MERIS channels

In figure 1, the transmission function of channel1 of the NOAA-K AVHRR/3 is presented together with the simulated transmission functions of MERIS channels 5 to 9 assuming Gaussian behavior.

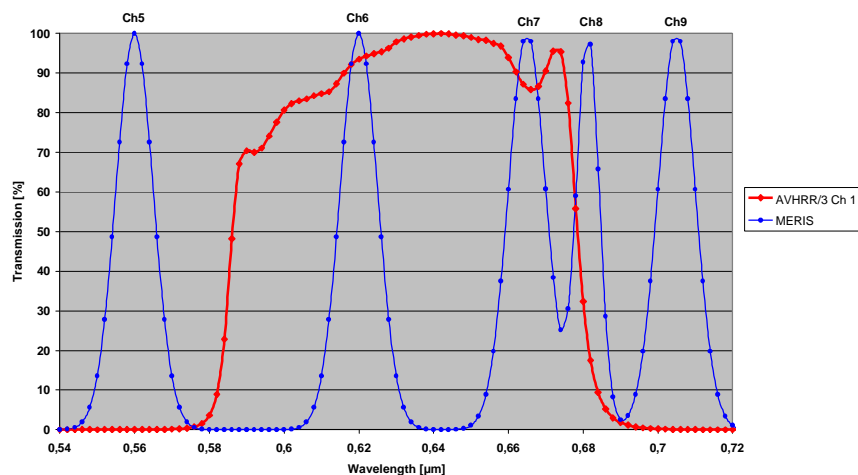


Figure 1. Transmission curves of NOAA-K AVHRR/3 and MERIS in the visible domain.

One can see that channel 6 and 7 of MERIS may fit to the AVHRR channel 1. Therefore, the following assumption is done:

$$\rho_1 = \alpha * (\rho_6^* + \rho_7^*)$$

In words, the reflectance detected by AVHRR in channel 1 can be approximated by a weighted sum of the reflectances detected by MERIS in channel 6 and 7. The weighting factor α will be determined by modeling the reflectances of different canopies under different observation geometries.

In figure 2, the transmission curve of channel 2 of NOAA-K / AVHRR/3 is presented together with the simulated Gaussian transmission functions of MERIS.

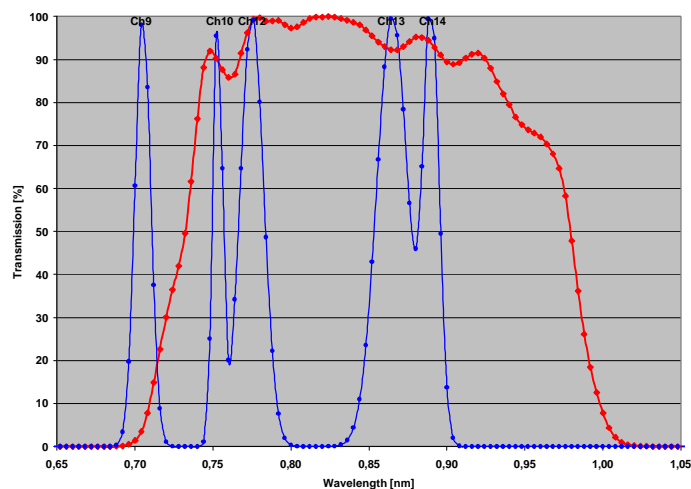


Figure 2: Transmission curves of NOAA-K AVHRR/3 and MERIS in the near-infrared domain.

Analogue to the previous statement, one can see that the MERIS channels 10,12,13,14 and 15 may fit to the AVHRR channel 2. MERIS channel 15 (not shown in figure 2) at 900 nm (with a bandwidth of 10 nm), which is positioned in the water vapor band, will also be taken into account due to the fact that the AVHRR_NDVI is based on not atmospherically corrected data. Therefore, the following assumption is done:

$$\rho_2 = \beta * (\rho_{10}^* + \rho_{12}^* + \rho_{13}^* + \rho_{14}^* + \rho_{15}^*)$$

In words, the reflectance detected by AVHRR in channel 2 can be approximated by a weighted sum of the reflectances detected by MERIS in channel 10 to 15. MERIS channel 11 located in the oxygen absorption band will not be included in this approximation due to the small bandwidth of 2.5 nm. Thus, the weighting factor β will be determined by modeling the reflectances of different canopies under different observation geometries.

Thus, for determining the weighting factors α and β a complex modeling is performed including the following steps.

- Determination of the relevant sun azimuth and sun zenith angles during a year for MERIS passes in the M1 grid
- Modeling the spectral reflectance and transmittance of single leaves using the SLOP model of Maier et al. (1999)
- Modeling canopy reflectance by applying an integrated canopy-leaf model based on the SAIL model of Verhoef (1984) and the SLOP model

	<h1>MERIS</h1>	Doc : MAPP-ATBD-NDVI Name : NDVI Issue : 1 Rev : 0 Date : 08/06/99 Page : 6
-----------------------------------------------------------------------------------	----------------	-----------------------------------------------------------------------------------------------------------------------------------

- Modeling canopy reflectance by varying leaf parameter (e.g. chlorophyll concentration, water status), canopy parameter (e.g. leaf angle distribution functions, LAI, structural parameter) and illumination and observation parameter (e.g. sun zenith angle, observation zenith angle, azimuth difference angle)
- Determining the “sensor-specific” reflectances for the two channels of NOAA-K AVHRR/3 and for the MERIS channels 6 to 15 and then determining the weighting factors α and β for each parameter set.

3.1.1.4 MERIS parameter and sun position

For a whole year the MERIS parameter describing the observation geometry in the M1 grid were calculated in steps of 35 days assuming an equator crossing at 8°30' (W) at 10:49:21 am (UTC). These data were found by running the software DESCW delivered by ESA. DESCW (Display Earth remote sensing Swath Coverage for Windows) is a multimission software tool to display coverage from different Earth Observation satellites (e.g. ERS-1, ERS-2, Landsat-5 and ENVISAT). The equator crossing time calculated by DESCW is not in agreement with other publications where one can find 10:00:00 am (UTC) for the descending node. But as one can see from the results later, this difference will not change the weighting factors α and β .

For determining the observation geometry, the following additional orbit parameter for ENVISAT are assumed:

Mean altitude:	799,8 km
Inclination:	98,55°
Repeat cycle:	35 days
Number of orbits in 1 cycle:	501
Time for one orbit:	100,6 minutes
Field of view for MERIS:	68.5 °
Earth radius:	6372 km

Starting with the equator crossing time, the sun and observation angles during a year were calculated for the M1 grid.

The M1 grid is defined as:

NW-point:	65° N, 12° W	NE-point:	65° N, 35° E
SW-point:	35° N, 12° W	SE-point:	35° N, 35° E

According to the repeat cycle of 35 days, the following Julian days are used for calculating the observation geometry and the sun position:

Day 1	1. January , day 36:	5. February, day 71	12. March, day 106	16. April,
day141	21. May, day 176	25. June, day 211	30. July,	
day 246	3. September, day 281	8. October, day 316	12. November and	
day 351	17. December.			

The general track of ENVISAT together with the eastern and western scan positions of MERIS for an equator crossing at 8°30' W is shown in figure 3.

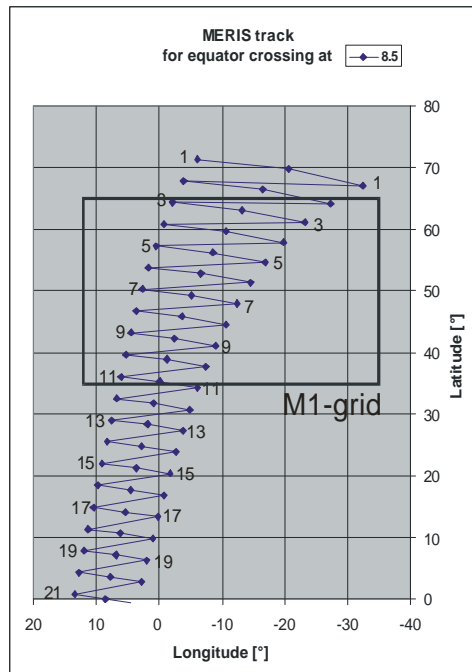


Figure 3: MERIS scan pattern over the northern hemisphere crossing the equator at 8°30' W. The M1 grid is also shown covering Europe. The longitude is negative for eastern positions. The numbers on each side of a scan indicate an arbitrary time interval in minutes.

One can see from figure 3, that the first scan within the M1 grid is scan 3 and the last scan within the grid is scan 11.

The sun position at Julian day 36 within the M1 grid is given in figure 4. For scan 3 one can see that the sun zenith angle for the nadir pixel is about 80°. Assuming that remote sensing of land surface becomes interesting for sun zenith angles lower than 60° (equivalent for 30° elevation) it can be seen that for day 36 the first scan fulfilling this requirement is scan 10. In terms of geographic position one must state, that the evaluation of MERIS data within the M1 grid starts at about 39° N. Valencia is located at ~39°N, 1° E.

The calculation gives for scan line 10 at day 36 a mean sun zenith angle of about 58° and an azimuth difference of 71° and 117°. The azimuth angles are calculated so that an azimuth angle of 180° represents south.

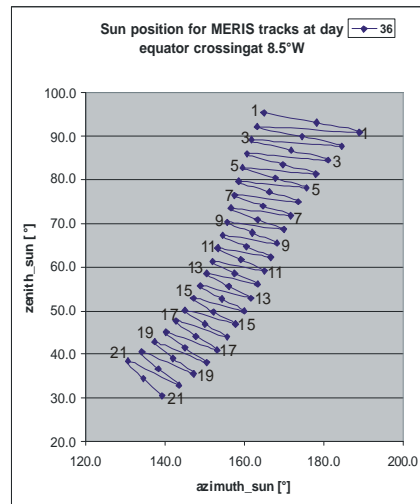


Figure 4 : Variation of the sun zenith and azimuth angle for Julian day 36. The numbers besides the scan lines indicate a relative time. The scan lines from number 3 to 11 are located within the M1 grid.

The relevant angles for the sun position as well as the observation geometry are calculated for 12 Julian days within one year. These results are input parameters for the calculation of canopy reflectances and the subsequent estimation of the weighting factors α and β .

3.1.1.5 Simulation of leaf reflectance

Leaf reflectance and leaf transmittance are modeled using the SLOP model (Stochastic model for Leaf Optical Properties) of Maier (1996). SLOP is based on the stochastic optical leaf model of Tucker and Garratt (1977) and the extended version developed by Luedeker and Guenther (1990). The extended model was revised, taking into account additional leaf components as e.g. the proteins, the lignins and in the future UV - protecting pigments located in the epidermal layer.

The extended model takes into account different mechanisms like absorption, reflection and scattering at the chloroplasts and the leaf cells as well as a new radiation state for the backscattered light from the spongy parenchyma. In addition the transition probabilities were modified.

With the revised Stochastic model for Leaf Optical Properties SLOP the reflection, transmission and absorption of light by leaves can be calculated in the spectral region from 400 nm up to 2.5 μm . The model treats the radiative transfer of diffuse light as transitions of light with weighted probabilities according to the theory of homogeneous Markov chains with a finite number of states. The leaves are divided in several compartments analogue to the well known leaf structure. A new radiation state is introduced for regarding the absorption in the epidermal layer, while in the palisade and spongy parenchyma the light is absorbed and scattered depending on their pigment concentration and the scattering efficiencies. The transition probabilities are determined by the optical properties of the leaf and the geometric leaf structure. The main parameters of the model are the concentrations and specific absorption coefficients of chlorophyll a and b, the accessory pigments (beta-carotene, lutein, violaxanthin, anthocyanin), proteins, cellulose, lignin and water. The specific absorption coefficients measured in alcoholic solutions are taken from the literature. The scattering coefficients and the thickness of the palisade and spongy parenchyma are also input parameters as well as the number of chloroplasts. The upper and lower epidermis is regarded as scattering element. Therefore the a priori knowledge of the reflectance spectrum is not necessary, in contrast to the commonly used semi-empirical models.

The model is now fully operational. The reflectance and transmittance spectra when changing the leaf parameter can be visualized in near real time. The algorithm is implemented as a macro function in an EXCEL sheet.

A typical result for the reflectance and transmittance of a green leaf is presented in figure 5. The chlorophyll a and b concentration is about $32 \mu\text{g} / \text{cm}^2$, the water equivalent thickness is 0.008 cm.

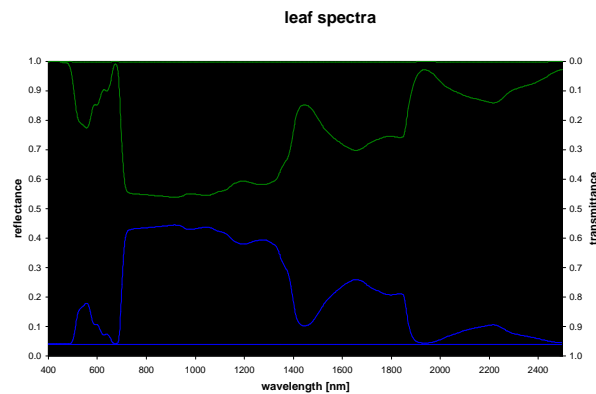


Figure 5: Reflectance (blue) and transmittance (green) of a green leaf, calculated by the SLOP model of Maier et al. (1999). The constant reflection is attributed to Fresnel reflectance at the leaf surface.

The reflectance and transmittance spectrum shown in figure 5 is used for modelling the canopy reflectance of green vegetation.

3.1.1.6 Simulation of canopy reflectance

In recent years many canopy radiative transfer models have been developed as e.g. the fast 2-stream model SAIL (Verhoef, 1984; Braswell et al., 1996), or on the other hand the highly complex 3-dimensional photon transport model 3-D DISORD (Myneni and Asrar, 1993), which is considered the most accurate but computationally expensive. The SAIL model is selected for modelling canopy reflectance since it produces nadir and off-nadir reflectance values with reasonable accuracy (e.g., Major et al., 1992; Huemmrich and Goward, 1997).

The SAIL model produces top-of-canopy reflectance values and needs the following input parameters:

- leaf area index (LAI)
- leaf angle distributions (LADF)
- leaf hemispherical reflectance $\rho_{\text{leaf}}(\lambda)$
- leaf transmittance $\tau_{\text{leaf}}(\lambda)$
- soil reflectance $\rho_{\text{soil}}(\lambda)$
- sun and view zenith and azimuth angles (Θ_{sun} , Φ_{sun} , Θ_{view} , Φ_{view}) and
- hot-spot parameter for each vegetation component ($\text{SIZE}_{\text{leaf}}$)

The hemispherical leaf reflectance and transmittance spectra will be calculated by the SLOP model which has the following inputs:

- pigment concentration (e.g. chlorophyll and carotenoids)
- water content
- leaf thickness including thickness of the palisade and spongy parenchyma and
- isotropic scattering coefficient in the leaf

In the past Jacquemoud et. al. (1995) inverted a coupled leaf – canopy transfer model (the PROSPECT – SAIL model) for extracting biophysical parameter of sugar beet from remote sensing data (AVIRIS and TM). Based on this work, we developed our coupled SLOP – SAIL model supported by S. Jacquemoud.

As an example, a variation of the observation zenith angle from -80° to 80° results in a variation of the reflectance at 805 nm from about 0.42 to about 0.80 while the other parameters (leaf reflectance and transmittance, soil reflectance, leaf angle distribution function, leaf area index, sun zenith angle and visibility) are fixed. The detailed results for different parameters of the canopy structure (“hot spot parameter”) are shown in figure 6 which can be used for comparison with the results of Jacquemoud et al (1995) presented in figure 2 of his paper.

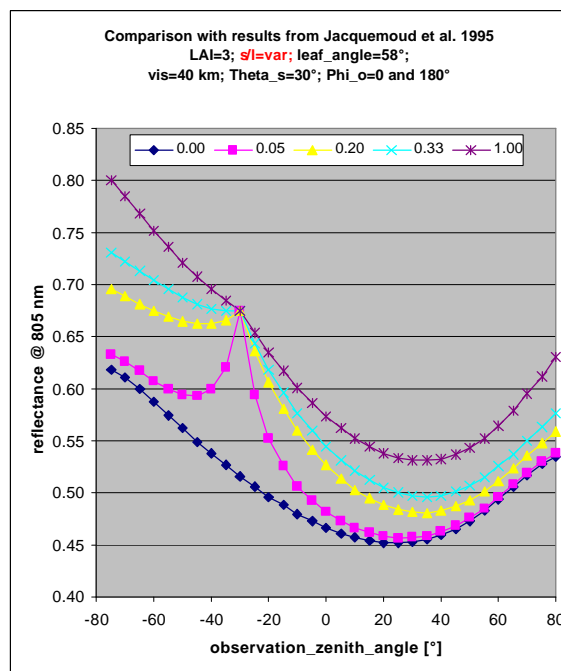


Figure 6: Variation of the canopy reflectance at 805 nm simulated by the coupled SLOP – SAIL model as a function of the observation zenith angle and the canopy structure parameter s/l (“hot-spot parameter”). s/l varies from 0 (no hot spot) to 1.

The reflectance functions of the coupled leaf-canopy model were used for calculating the signals for both sensors, AVHRR and MERIS. The simulation takes into account the transmission function of NOAA-K /-AVHRR3 and assumes Gaussian like transmission function for the MERIS channels.

From these sensor specific reflectance data, the weighting factors α and β were calculated for all input parameter sets (N ~3000) as described in section 3.1.2.3. The following results are found:

Weighting factor	Mean value	Standard deviation	Standard deviation [%]
α	0,2744	0,026103	9,51
β	0,0839	0,00061	0,73



3.1.1.7 Test of the correlation of MERIS_NDVI with AVHRR_NDVI

With the results for the weighting factors α and β as presented in the previous chapter the correlation of the MERIS_NDVI with the AVHRR_NDVI was calculated. For that purpose the coupled SLOP – SAIL model was running again with fixed weighting factors for determining the MERIS compatible NDVI.

For different leaf angle distribution functions the correlation between the MERIS_NDVI and the AVHRR_NDVI is calculated varying the leaf area index, the canopy structure parameter and the illumination and observation geometry which will be found during one year within the M1 grid (this means in general Europe).

In figure 7 the linear correlation between the modeled NDVI' s is demonstrated for a random leaf angle distribution.

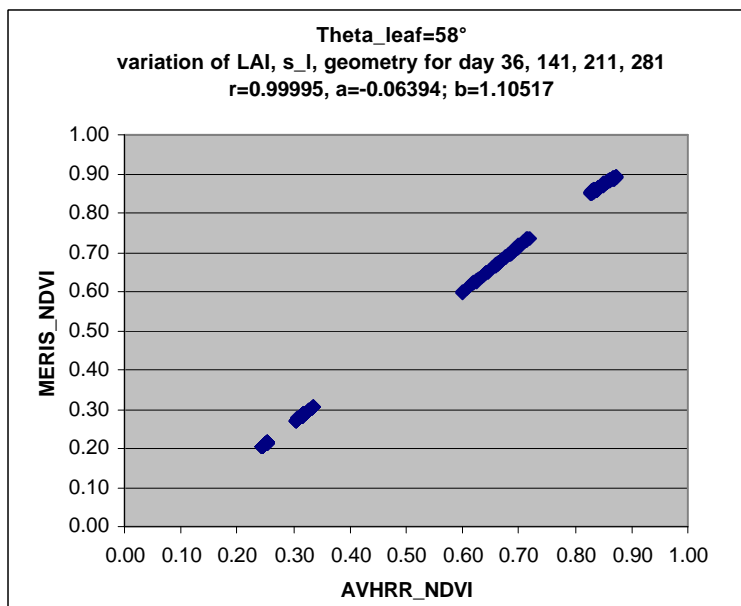


Figure 7: Correlation between the MERIS_NDVI and the AVHRR_NDVI applying weighting factors α and β of 0,2744 and 0,0839, respectively.

For different leaf angle distribution the correlation between the MERIS_NDVI and the AVHRR_NDVI changes only to a minor extent as can be seen from the following table. The leaf angle distribution function is parameterized by a mean angle and can be interpreted as follows:

LADF [°]	Interpretation	r	slope	intersection
15	Planophile	0,99997	1,10760	-0,06480
45	Plagiophile	0,99996	1,10583	-0,06419
58	Random	0,99995	1,10517	-0,06394
75	Erectophile	0,99991	1,10494	-0,06379

3.2 Practical Considerations

For implementation of the algorithm the following flow diagram (fig. 8) is taken as basis. MERIS level 1b data are read pixel by pixel together with the flags associated. When one of the following flags is set (sea, cloud, partly cloudy, cirrus or invalid) then no calculation is performed using the MERIS NDVI processor. Depending on the flags the NDVI for the pixel is set to zero (indication sea water or inland water) or is set to 255 indicating cloud, partly cloudy, cirrus or invalid. When no flag is set, the weighting factors α and β are used for calculating the AVHRR compatible NDVI according to the previous section.

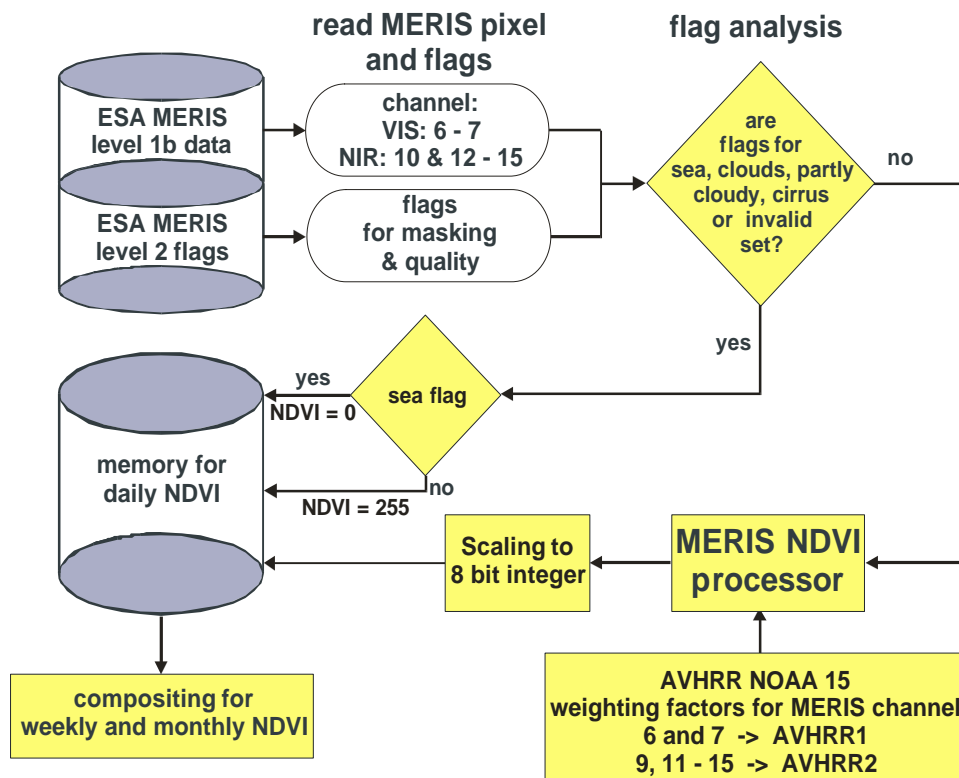


Figure 8: Flow diagram for the processing of MERIS level 1b data for calculating the AVHRR compatible MERIS_NDVI.

The MERIS_NDVI is then scaled to 8 bit integer thus that

$$1 < \text{MERIS_NDVI} < 254.$$

If the MERIS_NDVI is less or equal to -0.00996 then MERIS_NDVI=1. If MERIS_NDVI is greater or equal to 0.7 then MERIS_NDVI is set to 254.

	<h1>MERIS</h1>	Doc : MAPP-ATBD-NDVI Name : NDVI Issue : 1 Rev : 0 Date : 08/06/99 Page : 13
-----------------------------------------------------------------------------------	----------------	------------------------------------------------------------------------------------------------------------------------------------

3.2.1 Numerical computation considerations

The MERIS_NDVI is calculated as floating point value for every pixel. However, the scaling procedure transforms the MERIS_NDVI to 8 bit integer values. This is done for compatibility with the procedure supported by DFD when calculating the AVHRR_NDVI (see chapter 2.1).

3.2.2 Calibration and Validation

Pre-launch validation will be performed in 1999 using MOS data. For this purpose, MOS specific transmission functions must be applied to the results of the modeling activity in order to estimate the weighting factors α and β . With these weighting factors, some MOS scenes of Europe selected over one year will be processed and compared with AVHRR_NDVI products delivered by DFD.

Post-launch validation can only be performed when ENVISAT is in orbit and MERIS in operation.

3.2.3 Exception Handling

Exception handling will be performed according to the flags associated with MERIS level 1 b data as described previous.

3.2.4 Output Products

MERIS_NDVI will be given as an 8-bit-integer value. The following setting will be used:

The NDVI of water is set to 0. The NDVI of clouds, partly cloudy and cirrus is set to 255 as well as invalid pixels. The NDVI of other surfaces is in the range from 1 to 254.

NDVI = 1 is related to -0.00996
 NDVI = 254 is related to 0.7 and higher.

The weekly MERIS_NDVI is derived from daily MERIS_NDVI maps applying the maximum MERIS_NDVI algorithm to all daily maps available during a week. The maximum MERIS_NDVI algorithm is based on the evaluation of the maximum NDVI over the given time period on a pixel by pixel basis. This algorithm is also used for the production of monthly maximum maps. Water pixels are excluded from the algorithm as well as cloud pixels (NDVI=255).

4. ERROR BUDGET ESTIMATES

The calculations show very good correlation between the AVHRR_NDVI and the MERIS_NDVI when taking into account the variability of illumination and observation as well as the variability of different canopies and bare soil. For all modeling purposes done the agreement is better than $\pm 1\%$.

In order to be realistic, it should be noted that no atmospheric influence was regarded in the model.



5. REFERENCES

- Braswell, B.H., Schimel, D.S., Privette, J.L., Moore III, B., Emery, W.J., Sulzman, E.W., and Hudak, A.T. 1996. Extracting ecological and biophysical information from AVHRR optical data: an integrated algorithm based on inverse modeling, *J. Geophys. Res.* 101:23,335-23,345.
- Buschmann, C., and E. Nagel, 1993. *In vivo* spectroscopy and internal optics of leaves as basis for remote sensing of vegetation. *International J. Remote Sens.* 14: 711-722.
- Gitelson, A. A. and Merzlyak, M. N. 1996. Signature analysis of leaf reflectance spectra: algorithm development for remote sensing of chlorophyll. *J. Plant Physiol.*, 148, 495-500.
- Gitelson, A. A., Kaufman, Y. and Merzlyak, M. 1996. Use of a Green Channel in Remote Sensing of Global Vegetation from EOS-MODIS. *Remote Sensing of Environment*, Vol. 58, 289-298.
- Gitelson, A. A. and Merzlyak, M. N., 1994. Spectral reflectance changes associated with autumn senescence of *Aesculus hippocastanum* L. and *Acer platanoides* L. leaves. Spectral features and relation to chlorophyll estimation. *J. Plant Physiol.* 143, 286-292.
- Huemrich, K.F., and Goward, S.N. 1997. Vegetation canopy PAR absorptance and NDVI: an assessment for ten tree species with the SAIL model, *Remote Sens. Environ.* 61:254-269.
- Jacquemoud, S., Baret, F., Andrieu, B., Danson, F. M. and Jaggard, K., 1995. Extraction of vegetation biophysical parameter by inversion of the PROSPECT + SAIL models on the sugar beet canopy reflectance data. Application to AVIRIS and TM sensors. *Remote Sensing of Environment*, Vol. 52, 163-172.
- Lichtenthaler, H.K., Gitelson, A. A. and Lang, M. 1996. Non-destructive determination of chlorophyll content of leaves of a green and an aurea mutant of tobacco by reflectance measurements. *J. Plant Physiol.*, 148, 483-493.
- Luedeker, W., and Guenther, K.P. 1990. Leaf reflectance: A stochastic model for analyzing the blue shift, In: *Proc. Symp. on Global and Environmental Monitoring Techniques and Impacts*, Victoria BC (Canada), 17-21 September 1990, 28:475-480.
- Maier, S. W., Luedeker, W. and Guenther, K. P. 1999. SLOP: A Revised Version of the Stochastic Model for Leaf Optical Properties, accepted by *Remote Sensing of Environment*.
- Major, D.J., Schaalje, G.B., and Wiegand, C. 1992. Accuracy and sensitivity analyses of SAIL model-predicted reflectance of maize, *Remote Sens. Environ.* 41:61-73.
- Myneni, R.B., and Asrar, G. 1993. Radiative transfer in three-dimensional atmosphere-vegetation media, *J. Quant. Spectrosc Radiat. Transfer* 49:585-598.
- Sellers, P.J., 1985. Canopy reflectance, photosynthesis and transpiration, *Int. J. Rem. Sens.* 6:1355-1372.
- Tucker C. J., Justice C.O., Prince S.D., 1986. Monitoring the grasslands of the Sahel 1984-1985. *Int. J Remote Sensing* 7: 1571-1571.
- Tucker, C. J., and Garrat, M.W. (1977), Leaf optical system modeled as a stochastic process, *Appl. Opt.* 16:635-642.
- Vogelmann, Th. C., 1994. Light within the plant, In *Photomorphogenesis in Plants* (R. E. Kendrick and G. H. M. Kronenberg, Eds.) Kluwer Academic Publishers (The Netherlands), pp. 491-535.

 DLR	<h1>MERIS</h1>	Doc : MAPP-ATBD-NDVI Name : NDVI Issue : 1 Rev : 0 Date : 08/06/99 Page : 15
-------------------------------------------------------------------------------------------------	----------------	------------------------------------------------------------------------------------------------------------------------------------

Verhoef, W. 1984. Light scattering by leaf layers with application to canopy reflectance modeling: the SAIL model, *Remote Sens. Environ.* 16:125-141.

Yoder, B.J., and Waring, R.H., 1994. The normalized difference vegetation index of small Douglas-fir canopies with varying chlorophyll concentrations. *Remote Sens. Environ.* 49: 81-91.

6. MAPP DATA PRODUCT SUMMARY SHEET

Product name:	
Product code:	
Product Level:	
Description of the Product:	
Product Parameters:	
Coverage	
Packaging:	
Units:	
Range:	
Sampling:	
Resolution:	
Accuracy:	
Geo-location:	
Format:	
Appended data:	
Frequency of generation:	
Size of product:	
Additional information:	
Identification of bands used in algorithm	
Assumption on MERIS input data	
Identification of ancillary and auxiliary data	
Assumptions on ancillary and auxiliary data	

7. ACKNOWLEDGEMENT

We may thank Stefan Jacquemoud; University of Paris, France, very much, who supported our work by delivering his coupled PROSPECT-SAIL model. Based on this source code, we were able to develop our coupled SLOP-SAIL model in a very condensed form. The version is now running on PC's by calling macro functions in an EXCEL sheet.

We may also thank Mark Danson from the University of Salford, UK, for the development of a SAIL teaching model which is available for public use and was a good introduction to canopy reflectance.